1971

Thermal Conductivity of Heavily Doped P-Type Indium Antimonide at Liquid Helium Temperatures.

Charles Richard Crosby
Louisiana State University and Agricultural & Mechanical College

THERMAL CONDUCTIVITY OF HEAVILY DOPED p-TYPE InSb AT LIQUID HELIUM TEMPERATURES

A Dissertation

Submitted to the Graduate Faculty of the
Louisiana State University and
Agricultural and Mechanical College
in partial fulfillment of the
requirements for the degree of
Doctor of Philosophy

in

The Department of Physics and Astronomy

by
Charles Richard Crosby
B.S., Louisiana State University, 1957
M.S., Louisiana State University, 1960
May 1971

ACKNOWLEDGEMENTS

The author wishes to express his most sincere gratitude to Professor Claude G. Grenier for his guidance, assistance, and patience in the course of this experiment. Appreciation is extended to Dr. John T. Marshall for considerable assistance in the publication of this work.

Thanks are due to staff members Les Edelen, Fritz Overman, Phil Granata, Ed Keel, and Heinz Eichenseer for their assistance. Among the members and former members of the low temperature group, special thanks are due R. E. Hamburg, R. A. Herrod and P. M. Everett.

Financial assistance by the Atomic Energy Commission and the Charles E. Coates Memorial Fund of the L.S.U. Foundation donated by George H. Coates are gratefully acknowledged.

TABLE OF CONTENTS

	Page
Acknowledgements	ii
List of Tables	iv
List of Figures	v
Abstract	vi
Chapter	
I. Introduction	1
II. Experimental Details	3
III. Experimental Results	7
IV. Theory	12
V. Analysis and Discussion	27
VI. Conclusions	37
References	39
Vita	43

LIST OF TABLES

Table		Page
I.	Quantities determined from Hall effect and resistivity measurements	11
II.	Parameters determined from analysis of experimental data and some corresponding theoretical values	29

LIST OF FIGURES

Figure		Page
1.	The lattice thermal conductivity λ_g of three samples of heavily doped p-type InSb, multiplied by T^{-2} versus T in a linear plot.	8
2.	The lattice thermal conductivity of sample B, multiplied by T^{-2} versus T in a linear plot, showing the effects of screening of the charge carrier-phonon interaction for low q phonons.	31
3.	The sum τ^{-1} of the separate scattering frequencies, τ_b^{-1}, τ_c^{-1}, and τ_i^{-1} versus the magnitude of the phonon wave vector p in a log-log plot for sample B at $2^{o}K$ with $q_{TF} = q_{TF}^{e}$.	33
4.	The lattice thermal conductivity λ_g of five samples of heavily doped p-type InSb versus T in a log-log plot.	38

ABSTRACT

The lattice thermal conductivity, λ_g, of three heavily doped ($>10^{18}$ cm^{-3}) p-type samples of InSb has been determined in the temperature range 1.3 - 4.2°K. The data are fitted to a phenomenological model including boundary scattering, Rayleigh scattering due to impurities and isotopes, and the scattering of phonons by charge carriers. That the charge carriers are a significant source of scattering is indicated by a general T^2 behavior at the lowest temperatures and by a rapid increase in λ_g at the higher temperatures due to phonons which have wave propagation vectors larger than the diameter of the Fermi surface and which therefore cannot be scattered by charge carriers. A probable screening in the carrier-phonon interaction is apparent from the lowest temperature behavior of λ_g. In general, a good fit is made with the theories of charge carrier-phonon interaction developed for the treatment of ultrasonic attenuation.

I. INTRODUCTION

This work covers measurement and analysis of the thermal conductivity in heavily doped, degenerate p-type InSb in the liquid helium temperature range. This semiconductor was chosen as it was thought to present relatively isotropic electron and phonon distributions, thus allowing for more straight-forward analysis than in the case of Sb studied in a previous work.[1] Also, earlier work on InSb by Challis et al.[2] indicated that measurement of the electron-phonon scattering contribution to the thermal resistivity might be made possible by use of higher doping concentrations.

The principal features of the thermal conductivity which in this work would strongly confirm phonon scattering by charge carriers are: (a) a general tendency toward a T^2 dependence in the proper temperature range, (b) a rapid increase at the high temperature range similar to the effect of the cutoff in the phonon-electron interaction for phonons with wave propagation vector, q, larger than the diameter, $2k_F$, of the Fermi surface (FS) (The variation of $2k_F$ with the doping concentration allows some detailed study of this point.), (c) a departure from the T^2 dependence of the thermal conductivity at the lowest temperatures which would empirically agree with the screening[3] of the phonon-electron interaction in the regime of the long-wavelength phonons, and (d) a good fit with the relevant theories.

Theory[3-10] developed for the electron-phonon interaction in ultrasonic attenuation seems to adapt well for this case, and also

probably could explain some similar anomalies found in other heavily doped semiconductors.[11-13]

Chapter II is a brief description of the experimental procedure. Chapter III presents the experimental results. Chapter IV contains a development of the theoretical expressions to which the data are compared. Chapter V consists of an analysis of the results and a discussion of the thermal conductivity measurements. Chapter VI presents the conclusions drawn from this study.

II. EXPERIMENTAL DETAILS

The samples were purchased from Cominco American Incorporated.[14] They were rectangular parallelepipeds cut from heavily doped p-type single crystal InSb to have cross-section dimensions 2 x 4 mm and be as long as possible with the [111] axis perpendicular to within 5^{o} of the large face. Sample A was 22 mm long and doped with zinc. Samples B and C were doped with cadmium and had lengths of 30 mm and 28 mm respectively. The surfaces of the crystals as received were lapped.

The sample to be measured was soldered to a copper piece threaded on one end to screw into a copper heat sink which extended into the helium bath. A piece of 20 gage copper wire was wound with 44 gage insulated constantan wire, formed into a horseshoe shape, and the open end of the "horseshoe" soldered to the other end of the sample to serve as a heater. Thermometers and sample voltage leads were soldered to the large face of the crystal at points separated by between 6 and 9 mm depending on the length of the sample. All soldering to the sample was done with pure indium.

Electrical connections leading from the heater, from each of the thermometers, and from the sample into the helium bath were pairs of 40 gage formvar insulated superconducting niobium wire. Separate pairs of 36 gage formvar insulated copper wire were used as current and voltage leads from the bath to measuring apparatus for each of the thermometers and the heater. All other

electrical leads out of the dewar system also were 36 gage formvar insulated copper.

Temperature control was accomplished by regulating the vapor pressure above the helium bath. Two different regulators were required for this purpose and are described in detail by Long.[15] One regulator was used above the lambda point and a different one below the lambda point. Both regulators were backed by a Kinney type VSD vacuum pump.

The thermometers were a pair of Allen-Bradley 1/8 watt 51 ohm carbon resistors selected to have nearly identical temperature versus resistance characteristics. A thin coating of enamel had been removed to expose the carbon of the resistor, and Formvar insulated 38 gage copper wire was wound on this cylinder of carbon. The ends of the copper wire were brought together and twisted near the center of the resistor. The insulation was removed from this twisted lead which was then soldered to the sample.

A constant d.c. current of approximately 3 μa was supplied to each of the thermometers and the voltage across each was measured using a Leeds and Northrup[16] (L & N) type K-3 potentiometer with an L & N electronic null detector. Currents and voltages across the 250 ohm sample heater were measured with the same apparatus.

Calibration of thermometers was made immediately prior to the measurement of the thermal resistance by measuring the resistances of both thermometers at 4 or more temperatures each separated by approximately 10 m^{o}K with the sample heater turned off. The bath temperature was then lowered sufficiently such that when the

heater was turned on the temperature of the hot (nearest the sample heater) thermometer could be maintained by adjusting the heater current at the high temperature point of the calibration range while a temperature difference, ΔT, of between 10 and 40 $m^{o}K$ existed between the thermometers. Since the temperature of the hot thermometer was held constant, the temperature difference ΔT was simply the product of the slope, dT/dR, of the calibration curve and the change in resistance, ΔR, of the cold (nearest the heat sink) thermometer. The thermal conductivity is then given by

$$\lambda_g = \left(\frac{L}{A}\right) \frac{\dot{Q}}{\Delta T} \quad ,$$

where (L/A) is the ratio of the distance between the thermometer probes to the cross sectional area, and $\dot{Q}$ is the heat input rate to the sample by the heater.

The measurements of thermal conductivity were carried out in an evacuated enclosure which was evacuated to a forepump pressure of approximately 10^{-3} Torr at room temperature and then cryopumped as the sample enclosure (which contained some activated charcoal radiatively shielded from the sample) was submerged into the liquid helium bath.

The resistivity, Hall resistivity, and magnetoresistance were measured on all three samples. These were d.c. measurements carried out with the sample directly submerged in liquid helium. The longitudinal and transverse voltage probes were connected to a Rubicon[17] six dial thermofree potentiometer used as a precision

bucking/calibration voltage source. The output of the potentiometer was fed into a Keithley[18] model 147 nanovolt null detector used as a d.c. amplifier whose output was monitored on a strip-chart recorder. The magnetic fields for the Hall effect and magnetoresistance measurements were produced by a "home-made" iron core electromagnet with 10 inch diameter pole faces and a 8 inch gap capable of producing field strengths up to 13 $k0_e$.

III. EXPERIMENTAL RESULTS

The thermal conductivity of each of the three samples was measured as a function of temperature from $4.2^{\circ}K$ down to approximately $1.3^{\circ}K$. The data consist of between 15 and 25 separate temperature points for each sample at which two or more conductivity measurements were made.

The largest source of error in the data is a possible systematic error ($\approx$5%) in L, the thermometer probe separation, due to the size of the solder connections ($\approx$ .2 mm diameter) in relation to L. Other error occurs in the determination of the slope dT/dR of the thermometer calibration ($\approx$1%), the measurement of the resistance ($\approx$.5%), and measurement of the heat input to the crystal ($\approx$.2%).

The data are shown in Fig. 1.

The resistivity, Hall resistivity and magnetoresistance were measured in magnetic fields up to 8.6 $k0_e$ and at temperatures of $4.2^{\circ}K$ and $1.67^{\circ}K$ with no temperature dependence found in the electrical properties.

The valence band of InSb consists[19] of two approximately parabolic bands of very different curvature which are degenerate at the center of the zone. The ratio of the masses of the carriers in these two bands is of the order of 20,[19] with the heavy holes being the principal carrier.

For two bands of positive charge carriers the transverse or Hall resistivity in the low magnetic field limit can be written as

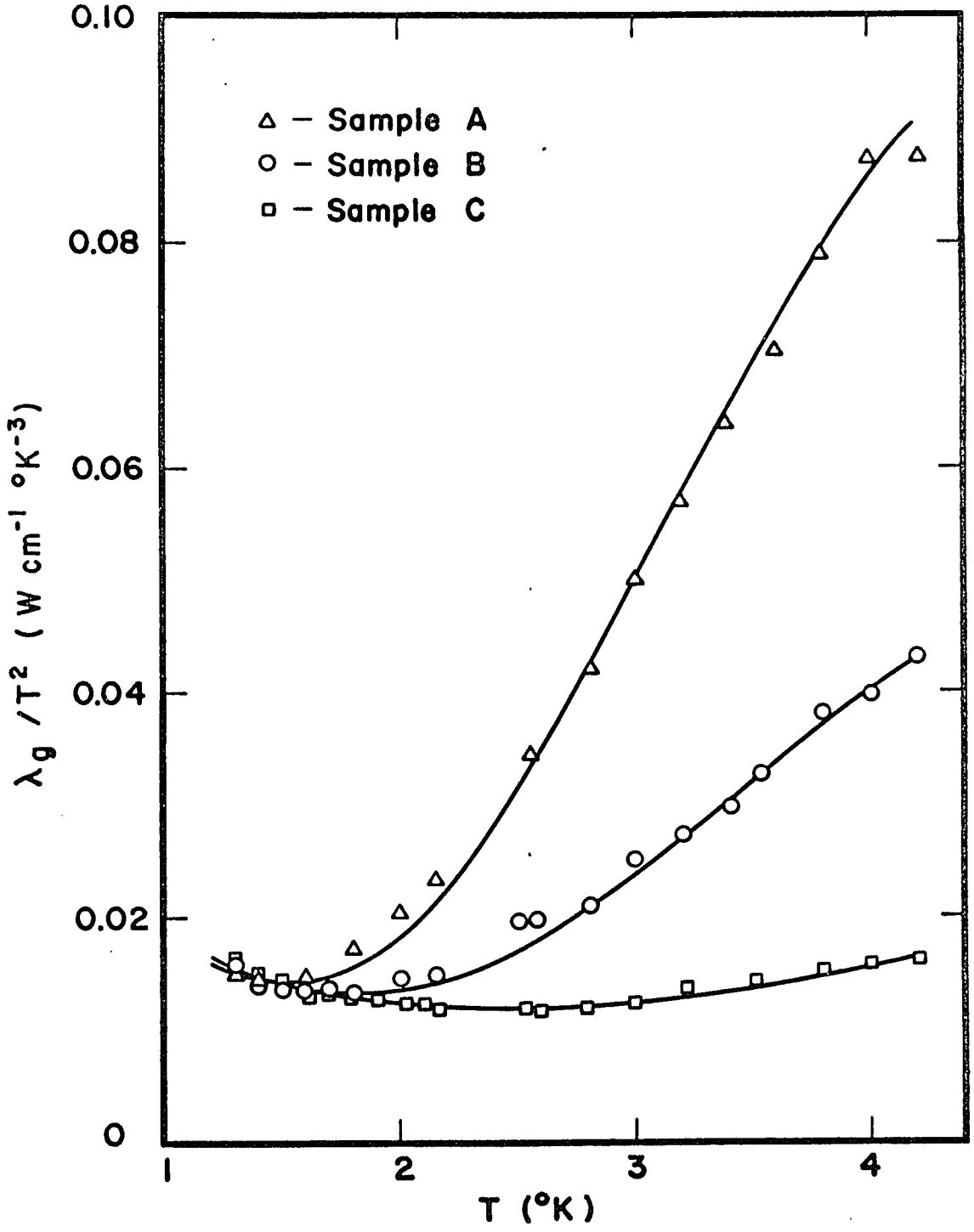
0.10
0.08
0.06
0.04
0.02
0
1
2
3
4
T (°K)
λ_g / T^2 (W cm^{-1} °K^{-3})
△ – Sample A
○ – Sample B
□ – Sample C

Fig. 1

$$\rho_{21} = \frac{H}{ec} \frac{(p_1\mu_1^2 + p_2\mu_2^2)}{(p_1\mu_1 + p_2\mu_2)^2} \quad ,$$

where the p_i and μ_i are the carrier densities and mobilities respectively. The total density of carriers is

$$p_1 + p_2 = R \frac{H}{ec\rho_{21}} = Rn \quad ,$$

where

$$R = \frac{(p_1\mu_1^2 + p_2\mu_2^2)(p_1 + p_2)}{(p_1\mu_1 + p_2\mu_2)^2}$$

is the ratio of the low field Hall coefficient to the high field Hall coefficient. By letting $\alpha = p_1/p_2$ and $\beta = \mu_1/\mu_2$ one can write

$$R = 1 + \frac{\alpha(\beta-1)^2}{(\alpha\beta + 1)^2} \quad ,$$

where it is easily seen that for R to approach unity either the mobilities of the separate bands must be nearly identical or, more practically, there must be orders of magnitude difference between the carrier densities. Several authors[20] have indicated that the ratio R for p-type InSb lies between 1.3 and 1.6. The value of the carrier density, n, used throughout this work is the value determined using R = 1 (which would correspond to the single band approximation generally used to characterize the carrier concentration in semiconductors) with the realization that this is an

underestimate in all calculations.

Using measured values of n and σ_o, the zero field conductivity, and assuming a value of the effective mass, m, one is able to calculate, in the isotropic parabolic single band approximation, values of the Fermi momentum $k_F = (3\pi^2 n)^{1/3}$, the Fermi energy $\epsilon_F = \hbar^2 k_F^2/2m$, the carrier lifetime $\tau_e = m\sigma_o/ne^2$, and the carrier mean-free-path $\ell_e = v_F \tau_e = \hbar k_F \sigma_o/ne^2$. Assuming an effective mass associated with the heavy hole valence band of 0.4 m_o[19] the quantities defined above were computed and are listed in Table I for each of the samples.

Table I

Quantities determined from Hall effect[20] and resistivity measurements. $n = H/ec\rho_{21}$, $\tau_e = m\sigma_o/ne^2$, $k_F = (3\pi^2 n)^{1/3}$, $\ell = \hbar k_F \tau_e/m$, and $\epsilon_F = \hbar^2 k_F^2/2m$ where ρ_{21} is the Hall resistivity, σ_o is the d.c. conductivity, and $m = 0.4m_o$ is the heavy hole effective mass.

Sample	n (10^{18} cm^{-3})	σ_o (ohm^{-1} cm^{-1})	τ_e (10^{-13} sec)	$2k_F$ (10^7 cm^{-1})	ℓ (10^{-6} cm)	ϵ_F (MeV)
A	1.08	136.0	1.8	1.01	1.65	24.0
B	2.20	218.0	1.4	1.16	1.64	32.0
C	7.60	537.0	1.0	1.51	1.77	54.0

IV. THEORY

The analysis of the experimental results uses an expression for the lattice thermal conductivity[25] in the limit of weak phonon mixing. This expression, assuming isotropy and linear dispersion in the phonon spectrum, is

$$\lambda_g = \frac{K}{2\pi^2 s} \left(\frac{KT}{\hbar}\right)^3 \int_0^{\theta/T} \tau \frac{x^4 e^x}{(e^x-1)^2} dx \ , \qquad (1)$$

where no distinction is made between transverse and longitudinal phonon modes. In eq. (1) s is an averaged value of the velocity of sound, $x = \hbar sq/KT$ where q is the magnitude of the phonon wave vector, τ is a q-dependent relaxation time and θ is the Debye temperature. At low temperatures where θ/T is large ($\theta \approx 200^{\circ}K$ for InSb[26]), the upper limit of the integral will be taken as infinite with negligible error.

When distinction between longitudinal and transverse sound waves is to be made under the same conditions as above, the conductivity is of the form,

$$\lambda_g = \frac{K}{6\pi^2} \left(\frac{KT}{\hbar}\right)^3 \int_o^{\infty} \left(\frac{\tau_L}{s_L} + \frac{2\tau_T}{s_T}\right) \frac{x^4 e^x}{(e^x-1)^2} dx \ , \qquad (2)$$

where the indices L and T refer to longitudinal and transverse modes respectively. In either case the phonon relaxation time, τ, is obtained assuming the principle of additivity of scattering frequencies as

$$\tau^{-1} = \tau_b^{-1} + \tau_c^{-1} + \tau_i^{-1} \quad , \tag{3}$$

where included are the scattering due to boundaries, charge carriers, and impurities respectively. All other mechanisms, including three-phonon processes, are neglected.

Boundary Scattering

The scattering relaxation frequency arising from crystal boundaries is given by the ratio of the velocity of sound, s, to the Casimir[27] length, L, and is a constant,

$$\tau_b^{-1} = B = s/L \quad . \tag{4}$$

The Casimir length for a sample of rectangular cross section of area S is such that $\pi L^2/4 = S$.

Impurity Scattering

The impurity scattering frequency, τ_i^{-1}, is somewhat complex and can be decomposed as the sum of terms,

$$\tau_i^{-1} = \tau_{iso}^{-1} + \tau_{i\cdot m}^{-1} + \tau_{i\cdot s}^{-1} + \tau_{i\cdot r}^{-1} + \tau_k^{-1} \quad . \tag{5}$$

The first three terms are Rayleigh type scattering, i.e. are proportional to the fourth power of the phonon wave vector, so that

$$\tau_{iso}^{-1} + \tau_{i\cdot m}^{-1} + \tau_{i\cdot s}^{-1} = Dq^4 = dx^4T^4 \quad , \tag{6}$$

where D is the constant of proportionality and $d = D(K/\hbar s)^4$. More specifically τ_{iso}^{-1} and $\tau_{i\cdot m}^{-1}$ are the mass difference scattering frequencies due to isotopes and substitutional impurities and are given by[11]

$$\tau_{iso}^{-1} + \tau_{i\cdot m}^{-1} = \frac{sq^4}{4\pi N^2} \sum_j N_j \left(1-M_j/\bar{M}\right)^2 = D_m q^4 \quad . \tag{7}$$

Here the summation is carried over all the kinds of molecules formed by the various isotopes and impurity atoms in the crystal. N_j and M_j correspond respectively to the number per unit volume and mass of a given kind of molecule, $\bar{M}$ is the average molecular mass, and N is the number of molecules per unit volume.

The other Rayleigh scattering term $\tau_{i\cdot s}^{-1}$ is a strain scattering caused by force constant difference and volume difference[28] associated with the impurities.

$$\tau_{i\cdot s}^{-1} = \frac{s}{2\pi N^2} \sum_j \left(\frac{\Delta F}{F} - \frac{4\Delta V}{V}\right)_j^2 = D_s q^4 \quad , \tag{8}$$

where N_j is the number of type j impurities and $\Delta F/F$ and $\Delta V/V$ are respectively the added stress and added dilatation introduced by the impurity. While D_m can be determined from Eq. (7), there is not sufficient information to calculate D_s. However, $D = D_m + D_s$ can be obtained experimentally from which one may estimate D_s.

A resonance scattering term $\tau_{i\cdot r}^{-1}$ of the type formulated by Pohl,[29]

$$\tau_{i\cdot r}^{-1} \propto \frac{\omega^2 T^n}{(\omega_o^2-\omega^2)^2 + (\Omega/\pi)^2\omega^2\omega_o^2} \quad ,$$

may modify the simple Rayleigh type behavior, but its effect is generally expected in a temperature range higher than the range reported here and therefore will not be considered. Here ω_o is the resonance frequency and Ω describes damping of the resonance, and n is a parameter which may be adjusted to fit experiment.

The last impurity scattering term of Eq. (5) is due to a resonance-like bound electron-phonon mechanism of the type proposed by Keyes,[30]

$$\tau_k^{-1} \propto \omega^4[\omega^2-(4\Delta/\hbar)^2]^{-2} \cdot [1+r_o^2\omega^2/4s^2]^{-8} \quad ,$$

where 4Δ is the chemical shift related to the splitting of electronic states and r_o is the mean radius of the localized state. If in p-InSb it is assumed that $\hbar\omega \ll 4\Delta$ the resonance term is eliminated. This scattering appears then to be of the Rayleigh type with a cutoff for $q > 2/r_o$ where r_o is the orbit radius of the electron or hole in the hydrogen-like state of the impurity. One may expect this cutoff to be concentration independent, and be well defined only for low impurity concentrations.

In summary the impurity scattering frequency can be approximated by a Rayleigh term $\tau_i^{-1} = Dq^4$. The deviation from this simple behavior due to $\tau_{i\cdot r}^{-1}$ and τ_k^{-1} will be neglected with some justification given in Section V. With this simplification, one notes that both the coefficient B of the boundary scattering and D

of the impurity scattering are proportional to s. Should distinction be made between longitudinal and transverse phonons, the corresponding B and D terms will be expected to be proportional to their corresponding velocities.

Charge Carrier-Phonon Scattering

Considering the scattering of phonons by charge carriers, either electrons or holes, Ziman[31] derived the relaxation time for the case in which the carriers are contained in a parabolic band and the density of carriers is large enough such that $T_F \gg T$, where the temperature T_F is defined by $KT_F = \hbar^2 k_F^2/2m$. Ziman showed that the scattering frequency is of the form

$$\tau_c^{-1} = \Omega_c(q) F_z(q) \quad , \tag{9}$$

where $F_z(q)$ is a cutoff function which takes account of the fact that due to momentum and energy conservation not every phonon can be scattered. When the carrier is scattered from a state characterized by a vector $\vec{k}$ to a state $\vec{k}'$ with $\vec{k}' = \vec{q} + \vec{k}$, the condition $q \leq 2k_F$ is imposed on q due to the upper limit k_F taken by both k and k', where k_F is the Fermi radius. It is expected that the function $F_z(q)$ would decrease from unity to zero rather sharply in the vicinity of $2k_F$. This is what is realized by the Ziman cutoff function. Taking into consideration both energy and momentum conservation the function $F_z(q)$ takes the form

$$F_z(q) = 1 - \frac{kT}{\hbar qs} \ln \frac{1 + \exp \frac{1}{KT}\left[\frac{\hbar qs}{2} - \frac{\hbar^2}{8m}(4k_F^2 - q^2)\right]}{1 + \exp \frac{1}{kT}\left[-\frac{\hbar qs}{2} - \frac{\hbar^2}{8m}(4k_F^2 - q^2)\right]}$$

or

$$F_z(x) = \frac{1}{x} \ln \frac{\exp(\frac{x}{2}) + \exp\left[-\frac{T}{16T_s}((\frac{\theta^*}{T})^2 - x^2)\right]}{\exp(-\frac{x}{2}) + \exp\left[-\frac{T}{16T_s}((\frac{\theta^*}{T})^2 - x^2)\right]} \qquad (10)$$

where m is the effective mass of the carrier and

$$\theta^* = 2k_F(\frac{\hbar s}{K}) = \sqrt{4T_F T_s} \qquad (11)$$

is a parameter of interest to characterize low temperature transport effects.[32] The temperature T_s is defined by $KT_s = ms^2/2$.

The scattering function $\Omega_c(q)$ is taken by Ziman to have the simple form

$$\Omega_c(q) = Aq = axT \quad , \qquad (12)$$

with $A = m^2C^2/2\pi\rho\hbar^3$ and $a = Km^2C^2/2\pi\rho s\hbar^4$ where C is the deformation potential and ρ is the mass density.

It is generally argued that the local strain induced by the sound wave changes the energy of the charge carriers by the amount

$$\delta E(r) = \sum_{ij} C_{ij}\Delta_{ij}(r) \quad , \tag{13}$$

where the C_{ij} are the components of the deformation potential tensor and the $\Delta_{ij}(r)$ are the components of the local strain. The value of C occurring in the coefficients of Eq. (12) is a scalar assumed independent of the phonon polarization or crystal orientation.

When an analysis of the conductivity is made using the expressions (1), (3), (4), (6), (9), (10), and (12) with proper adjustment of the parameters C, d, and θ^*, a relatively good fit is obtained at the highest temperatures concurring to the evidence of the Ziman cutoff of the carrier scattering. However, at the low temperature end there are indications that the simple linear term $\Omega(q) = Aq$ overestimates the scattering of the low q phonons. This is to be expected from qualitative considerations. When the phonon wave-length becomes of the order of or larger than the carrier mean free path, i.e. $q\ell \lesssim 1$, the decrease in the strength of the interaction which occurs in metals may also exist in semimetals. Moreover, one realizes that the electron system reacts as a plasma to low frequency phonons, and the resulting screening decreases the charge carrier-phonon interaction.

A number of theories have been developed in the field of acoustic attenuation which have these features. One such theory is the one by Cohen et al.[3] with the extensions of Harrison[4] and Spector[5] (CHS). CHS treats the conducting solid as a gas of n charge carriers per unit volume moving through a uniform background of

opposite charge of the same density. The acoustic wave manifests itself as a velocity field $u(\vec{r},t) \propto \exp[i(\vec{q}\cdot\vec{r}-\omega t)]$.

CHS calculates the attenuation coefficient which is the power density dissipated per unit energy flux. The carrier scattering frequency is equal to the product of the attenuation coefficient and the sound velocity. For the InSb samples studied here the resultant carrier scattering frequency depends only on terms involving the square of the deformation potential tensor components to within 1%. This was determined by numerical calculations based on the equations of CHS using parameters for InSb listed in Table I. If only terms involving the square of the deformation potential are important then the ionic currents can be neglected. This would signify that the results are independent of carrier compensation, i.e. whether compensation is assumed or not will have no effect on terms which involve the square of the deformation potential tensor. This allows one to approach the derivation of the scattering frequency along the lines presented by S. G. Eckstein,[10] whose treatment results in expressions which are more applicable to the problem at hand.

Eckstein proceeds in essentially the same way as CHS by first writing the equation for the self-consistent field as

$$\vec{j}_s = -\hat{B} \cdot \vec{E}_s \quad . \tag{14}$$

Here $\vec{j}_s$ and $\vec{E}_s$ are those components of the current and field which vary like the velocity field, $\vec{u} \propto \exp[i(\vec{q}\cdot\vec{r} - \omega t)]$. If the 1 direction is chosen along $\vec{q}$, $\hat{B}$ is the diagonal tensor with

components $B_{11} = -i\gamma$ and $B_{22} = B_{33} = i(c/s)^2\gamma$ where $\gamma = \epsilon\omega/4\pi$; ϵ is the static dielectric constant of the solid, c the velocity of light, s the velocity of sound, and $\omega = qs$. The current $\vec{j}_s$ is the sum of all a.c. currents which may arise, i.e. from additional carrier bands, and are obtained from distribution functions which are solutions to Boltzman's equation.

Assuming two compensated conducting bands the current is

$$\vec{j}_i = \hat{\sigma}_i \cdot (\vec{E}_s - \vec{q}\vec{q} \frac{\hat{C}_i \cdot \vec{u}}{i\epsilon\omega} + \frac{m_i \vec{u}}{e\tau_i}) + \vec{R}_i n_i' e s \ , \qquad (15)$$

where the subscript i refers to the band and is either 1 or 2 and e is the charge of the carrier including sign. Here τ_i is the carrier lifetime and m_i the carrier mass in band i,

$$\hat{\sigma}_i = e\tau_i \int \frac{(-\partial f_o/\partial E)\vec{v}\vec{v} d^3v}{1 - i\omega\tau_i + i\vec{q}\cdot\vec{v}\tau_i} \ , \qquad (16)$$

and

$$\vec{R}_i = \frac{2\epsilon_F}{3n_i s} \int \frac{(-\partial f_o/\partial E)\vec{v} d^3v}{1 - i\omega\tau_i + i\vec{q}\cdot\vec{v}\tau_i} \ . \qquad (17)$$

Here $f_o = f_o(E, \epsilon_F, T)$ is the equilibrium Boltzman distribution function where ϵ_F is the Fermi energy, and E the carrier energy.

The conductivity tensor, $\hat{\sigma}_i$, which contains most of the information concerning forces and fields is diagonal with components

$$\sigma_{i11} = 3\sigma_i^{o}\left(\frac{1-i\omega\tau_i}{(q\ell_i)^2}\right)p_i, \quad \sigma_{i22} = \sigma_{i33} = \frac{3\sigma_i^{o}}{2}\left[\frac{1-p_i}{1-i\omega\tau_i} - \frac{(1-i\omega\tau_i)p_i}{(q\ell_i)^2}\right], \tag{18}$$

where σ_i^{o} is the d.c. conductivity of band i and

$$p_i = 1 - \frac{1}{2}\int_{-1}^{1}\left[1-iq\ell_i(1-i\omega\tau_i)y\right]^{-1}dy \quad . \tag{19}$$

Here ℓ_i is the carrier mean free path in band i. The quantity $\vec{R}_i$ comes about due to diffusion of the nonuniform part of the carrier density, n_i', which can be related to the current in the direction of propagation of the sound wave by means of the equation of continuity as

$$j_{i1} = -n_i' es \quad . \tag{20}$$

Actually there are other possible sources of current divergence such as recombination, ionization or carrier trapping not taken into account in arriving at Eq. (20), but this can be taken into account by simply introducing a coefficient[33] α into the right side of Eq. (20).

For convenience one may define the tensor, $\hat{R}_i$, by the equation

$$\hat{R}_i \cdot \vec{j}_i = \vec{R}_i j_{i1} \ , \tag{21}$$

where the only nonzero component of $\hat{R}_i$ is the 11 component which is $p_i/i\omega\tau_i$. The current equations (Eq. (15)) may then be written

$$\vec{j}_i = \hat{\sigma}_i' \cdot \left[\vec{E}_s - \vec{q}\vec{q} \frac{\hat{C}_i \cdot \vec{u}}{ie\omega} + \frac{m_i \vec{u}}{e\tau_i}\right] \quad , \tag{22}$$

where

$$\hat{\sigma}_i' = \left[\hat{I} - \alpha \hat{R}_i\right]^{-1} \hat{\sigma}_i \quad . \tag{23}$$

The sound wave supplies energy to the charge carriers as it propagates and this energy is dissipated to the neutral background through collisions. It can be shown[4] that the power dissipated per unit volume from the sound wave is given by

$$Q = \frac{1}{2} \text{Re } \vec{u}^* \cdot \left[(\hat{C}_1 - \hat{C}_2) \frac{\vec{q}\vec{q}}{2ie\omega} (\vec{j}_1 + \vec{j}_2) - (\hat{C}_1 + \hat{C}_2) \frac{\vec{q}\vec{q}}{2ie\omega} (\vec{j}_1 + \vec{j}_2)\right.$$

$$\left. + \frac{m_1 \vec{j}_1}{e\tau_1} - \frac{m_2 \vec{j}_2}{e\tau_2} + n\left(\frac{m_1}{\tau_1} + \frac{m_2}{\tau_2}\right)\vec{u}\right] \quad , \tag{24}$$

where $\vec{u}^*$ is the complex conjugate of $\vec{u}$ and $n = n_1 = n_2$ is the carrier density in either band.

The scattering frequency for the charge carriers is given by the product of the velocity of sound and the attenuation coefficient. The latter is simply the energy dissipated per unit energy flux or

$$\Omega(q) = s\alpha_{\text{atten.}} = s \frac{Q}{\frac{1}{2}\rho |\vec{u}|^2_s} \quad , \tag{25}$$

where ρ is the mass density of the solid.

Neglecting terms independent of the square of the deformation

potential and assuming that the sound wave is propagating in the 1-direction and is polarized in either the 1- or 2-direction one can write after substituting Eqs. (14), (22) and (24) into (25),

$$\Omega(q) = \frac{-q^4}{\rho e^2 \omega^2} \mathrm{Re} \frac{\sigma_1'\sigma_2'(C_1 \pm C_2)^2 + B(\sigma_1' C_1^2 + \sigma_2' C_2^2)}{\sigma_1' + \sigma_2' + B}. \quad (26)$$

Here B and the σ_i' are now the 11 components of the respective tensors and the C_i are either the 11 or the 12 components of the deformation potential tensor depending on whether longitudinal or transverse phonons are being considered.

The limiting forms for Eq.(26) for a single conducting band, i.e. for $\sigma_2' = 0$, are

$$\Omega_L(q) = \frac{-q^2}{\rho e^2} \left(\frac{C_{11}}{s_L}\right)^2 \Sigma(q, s_L)$$

$$\Omega_T(q) = \frac{-q^2}{\rho e^2} \left(\frac{C_{12}}{s_T}\right)^2 \Sigma(q, s_T) \quad , \quad (27)$$

where

$$\Sigma = \mathrm{Re}\left(\frac{\sigma_{11}' B_{11}}{\sigma_{11}' + B_{11}}\right) \quad (28)$$

is the reduced conductance of the two impedances $1/\sigma_{11}'$ and $1/B_{11}$ in series. As indicated earlier $B_{11} = -i\epsilon\omega/4\pi$, whereas σ_{11}' can be obtained from Eqs. (18) and (23) and is

$$\sigma_{11}' = \frac{3\sigma_o \omega\tau_e (1-i\omega\tau_e)p_e}{(q\ell)^2(ip_e+\omega\tau_e)} \quad , \tag{29}$$

where p_e is given by Eq. (19). It is interesting to note that the scattering terms in Eq. (27) exhibit the same q dependency as opposed to the case of metals where the scattering frequencies for the different phonon polarizations appear as completely different functions of the phonon wave vector. In the range of interest here one finds by numerical calculation using Eqs. (28) and (29) with values of σ_o, τ_e and ℓ given in Table I and $\epsilon = 18$.[19] $\Sigma_L/\Sigma_T \simeq (s_L/s_T)^2$, thus

$$\frac{\Omega_L(q)}{\Omega_T(q)} = \left(\frac{C_{11}}{C_{12}}\right)^2 \quad .$$

Since the total relaxation frequencies for longitudinal and transverse modes differ only in the carrier scattering term, and since these terms are shown to have the same q-dependency and since C_{11} and C_{12} are of the same order, it is felt that this is an indication that the analysis based on Eq. (1) where no distinction is made between longitudinal and transverse mode is a relevant approximation and that the empirically determined scattering in this simplified analysis will be representative of the basic scattering involved in the InSb samples studied. More specifically when

$$\ell^{-1} < q_{TF} < q < 2k_F \tag{30}$$

where $q_{TF} = \omega_p/v_F$ is the Thomas-Fermi wave vector and v_F is the Fermi velocity of the carriers, the value Σ simplifies and Eq. (27) yields the term used in Ziman's theory for $\Omega(q)$, i.e. Eq. (12).

If the phonon-charge carrier scattering is preponderant over τ_b^{-1} and τ_i^{-1} and if one considers the temperature range where contribution to the heat conduction comes mostly from phonons satisfying condition (30), it is expected that the lattice thermal conductivity λ_g will exhibit the usual T^2 law,

$$\lambda_g = \frac{7.212\hbar K^3 \rho}{\pi m^2} C^{-2} T^2 \tag{31}$$

or

$$\lambda_g = \frac{7.212\hbar K^3 \rho}{\pi m^2} \left(\frac{1}{3} C_{11}^{-2} + \frac{2}{3} C_{12}^{-2}\right) T^2 \quad .$$

These were obtained from Eqs. (1) and (2) respectively where

$$\int_o^\infty \frac{x^3 e^x dx}{(e^x-1)^2} = 7.212 \quad .$$

Therefore, it may be seen that the average over modes yields for the averaged deformation potential the relation,

$$C^{-2} = \frac{1}{3} C_{11}^{-2} + \frac{2}{3} C_{12}^{-2} \quad . \tag{32}$$

The components of the deformation potential in fact depend on the direction in which q is taken in the crystal. However, the

calculation of λ_g involves an averaging over all q directions so that the C_{11} and C_{12} appearing in Eq. (32) may be considered as averaged quantities.

Outside of the $\lambda_g \approx T^2$ range the situation is more complex. At the higher temperatures where phonons with $q \approx 2k_F$ have to be considered, Ziman's cutoff, $F_z(q)$, as expressed as a function of x in Eq. (2) occurs for different values of x, θ_L^*/T, and θ_T^*/T for the different polarizations. Therefore, in the simplified analysis where a single cutoff is used instead of two, some indetermination will result mainly in the averaged impurity scattering term. The impurity scattering is indeed the principal scattering once the carrier scattering is cut off. It is questionable whether or not the refinement made by inclusion of the double cutoff might be offset by the ambiguity in the determination of the θ^* due to anisotropy in the phonon and electron distributions.

At lower temperatures where phonons with $q \approx q_{TF}$ have to be considered, the Σ function takes a complicated form which nevertheless simplifies if $q\ell \gg 1$ for which the scattering becomes

$$\Omega(q) = Aq\left[1 + 3(q_{TF}/q)^2\right]^{-2} \tag{33}$$

which is a conveniently simple formulation of the plasma screening cutoff. Thus for $q > q_{TF}$ the scattering approaches the unscreened term given by Eq. (12), whereas for $q < q_{TF}$ the screening effect for small q makes the carrier scattering term fall sharply.

V. ANALYSIS AND DISCUSSION

In the analysis of the conductivity it was felt that the simple form of Eq. (1), where no distinction between phonon polarization is made, could be used to determine the nature of scattering, subject to the restrictions discussed above. An averaged value for the velocity of sound $s = 2.26 \times 10^5$ cm/sec[26] is used in the different computations, except when specific dintinction between polarizations is made in the discussion, in which cases s_L and s_T averages are taken as $s_L = 3.77 \times 10^5$ cm/sec and $s_T = 1.88 \times 10^5$ cm/sec.[26] The mass density $\rho = 5.775$ gm cm^{-3} is used.[26] The values for n, τ_e, and ℓ are taken from Table I. The hole mass used is $m = 0.4\ m_o$[19] and the static dielectric constant $\epsilon = 18$.[19] From those basic quantities, one can derive such quantities[20] as k_F, θ^*, θ_L^*, θ_T^*, v_F, ω_p, $q_{T.F}$ for the different samples as well as D_m if one supposes the impurity density is given by $N_i = n$. Using Eqs. (3), (4), (6) and (9) one obtains for the relaxation frequency

$$\tau^{-1} = B + Dq^4 + \Omega(q)F_z(q)$$

where $F_z(q)$ is given by Eq. (10) and $\Omega(q)$ is represented by

$$\Omega(q) = \frac{q^2}{\rho e^2}\left(\frac{C}{s}\right)^2 |\Sigma(q,s)| ,$$

where Σ is given in Eq. (28). In principle only C and $d = D(K/\hbar s)^4$ are unknown quantities which may be adjusted and used in Eq. (1) to fit the experimental data for λ_g. However, it was found that a very good fit with the data was achieved when the additional quantities θ^* and q_{TF} are treated as parameters and properly adjusted. θ^* enters through $F_z(q)$ as shown in Eq. (10), whereas q_{TF} enters through Eq. (28) since $B_{11} = -i\sigma_o\omega/\omega_p^2\tau_e$, where $q_{TF}=\omega_p/v_F$. Then comparison between experimental and computed values for these parameters would serve as a check into the theory and the validities of the approximations.

The values of C, d, θ^* and q_{TF} obtained for a best fit are presented in Table II along with calculated values[20] of θ^*, d_m, and q_{TF} for each sample. The results of the calculation of λ_g using the values in Table II are represented by the solid curves which accompany the experimental data points in Fig. 1. The way in which the individual sets of data break away from the low temperature nearly T^2 dependence of λ_g is indicative of the abrupt cutoff in scattering by charge carriers of phonons with $q > 2k_F$. The sequence in which these cutoffs occur follows the sequence of increase of $2k_F$ due to increased doping. The somewhat less than T^2 behavior at the lowest temperatures is attributed to screening of the charge carrier-phonon interaction for low q phonons. The solid curves are computed from Eq. (1) using parameters listed in Tables I and II.

The curves fit to the experimental data are quite sensitive to the deformation potential since it is the principal parameter

TABLE II

Parameters $|C|$, d, θ^* and $q_{TF}{}^e$ determined from analysis of data using Eq. (1) along with calculated values of d_m, $\theta_{CALC}{}^*$, and $q_{TF}{}^c$. Here $q_{TF}{}^e$ is the value arising from the curve fit and $q_{TF}{}^c$ is the theoretical value of the Thomas-Fermi wave vector calculated from the relation $q_{TF} = \omega_p/v_F$ where ω_p is the plasma frequency and v_F is the Fermi velocity.

Sample	$\|C\|$ (eV)	d ($^oK^{-4}$ sec^{-1})	d_m ($^oK^{-4}$ sec^{-1})	θ^* (^oK)	$\theta_{CALC.}{}^*$ (^oK)	$q_{TF}{}^e$ (10^6 cm^{-1})	$q_{TF}{}^c$ (10^6 cm^{-1})
A	+1.18	13.5	3.2	17.5	11.0	0.82	2.38
B	+1.12	20.0	2.8	20.0	14.0	0.80	2.68
C	+1.06	25.0	2.9	26.0	21.1	0.75	3.29

which determines the depth of the minimum for the λ_g/T^2 versus T curve. The values of the deformation potential obtained are within the range expected.[11,34] There seems to be a slight dependency of the deformation potential on the impurity concentration, with the magnitude of C decreasing as n increases.

The effective Debye temperatures, θ^*, resulting from the analysis are in the same sequence, but are larger than the values calculated from the measured carrier densities. As mentioned earlier, the θ^* for each sample should probably not be a single value but take on a range of values between θ_T^* and θ_L^*. The θ^* obtained experimentally for all three samples are in the range between the calculated values for θ_T^* and θ_L^* and should the correction implied in ref. (20) be performed a still better match would be obtained. The analysis is reasonably sensitive to θ^* as this parameter located the minimum along the temperature axis and in conjunction with the parameter d determined the slope above the minimum.

The introduction of the Thomas-Fermi wave vector as a parameter allows control of the amount of screening by delaying the onset of screening as q_{TF} is decreased. That some control over screening is necessary is indicated in Fig. 2 where the data for sample B are presented along with solid curves representing best fits using the carrier scattering represented by Eq. (12) where there is no screening (curve 1), CHS with the full effect of screening (curve 3), and CHS with the screening reduced by adjustment of q_{TF} (curve 2). Curve 3 uses Eq. (1) with parameters listed in Tables I and II with

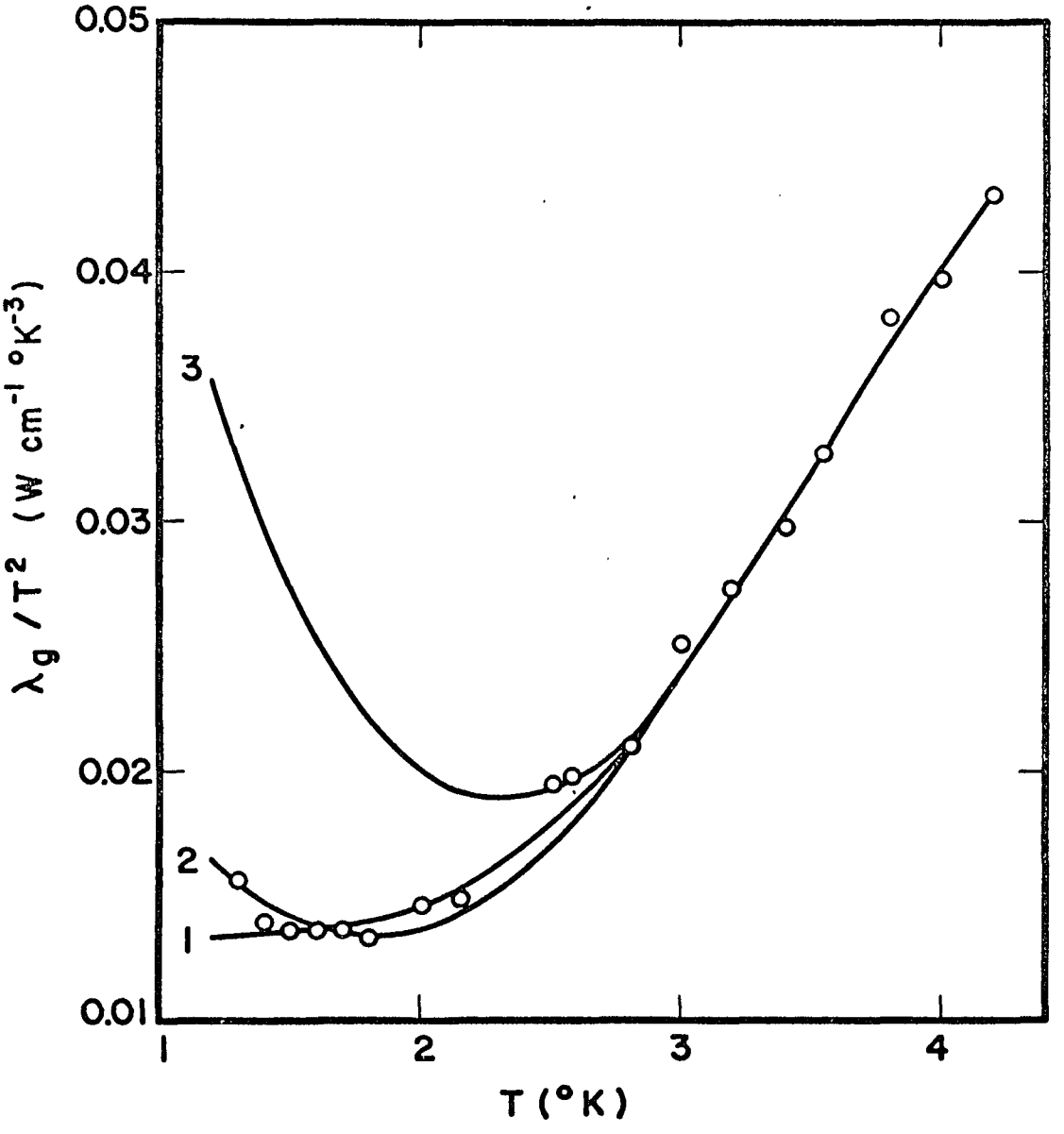

Fig. 2

the value of q_{TF}^{c} which introduces the full theoretical effects of screening. Curve 2 was computed exactly as curve 3 with the exception that q_{TF} was adjusted to the value of q_{TF}^{e} to reduce the screening. Curve 1 is a fit to the data with no screening. The parameters for this curve were adjusted to give a best fit and are somewhat different than for curves 2 and 3. Table II shows that the values of q_{TF} obtained by curve fitting are much smaller than those calculated, varying from 34% of the expected value for sample A to only 23% for sample C. By comparison Challis #6 sample with less doping yields 42%. It may be noted that the purer the sample the closer to the theoretical expectation for q_{TF}. Attempts to explain such a small empirical value of the parameter used in place of the Thomas-Fermi wave vector will be made later.

To illustrate the different types of phonon scattering as obtained for sample B, the phonon scattering frequencies due to the three principal scattering mechanisms are shown in dashed lines in Fig. 3 as functions of the phonon wave vector with the sum of the scattering frequencies as the solid curve. In this figure the carrier scattering displays the very rapid fall due to screening when the phonon wave vector is of the order of q_{TF}^{e} or less. Other features apparent in this figure are the very abrupt cutoff of charge carrier scattering at $2k_F$ as calculated for $T = 2^{o}K$ and the linear wave-vector dependence of the carrier scattering frequency for $q > q_{TF}$ which agree with the Ziman theory. The boundary scattering appears as the term independent of q.

It can easily be seen that an increase in the scattering due

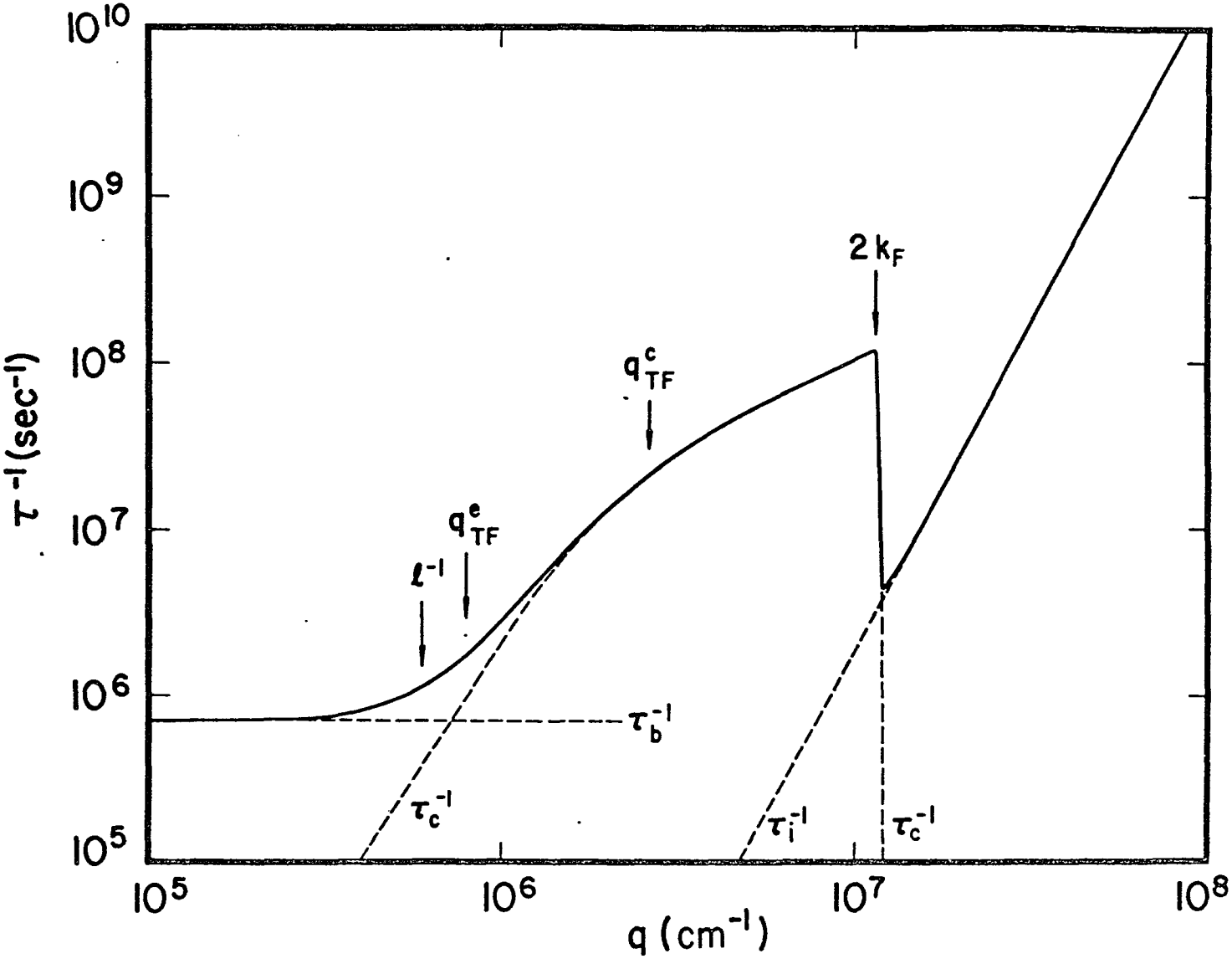
10^{10}
10^{9}
10^{8}
10^{7}
10^{6}
10^{5}
$\tau^{-1}(sec^{-1})$
$2k_F$
q^c_{TF}
q^e_{TF}
ℓ^{-1}
τ_b^{-1}
τ_c^{-1}
τ_i^{-1}
τ_c^{-1}
10^5
10^6
10^7
10^8
$q\ (cm^{-1})$

Fig. 3

to crystal boundaries would compensate in part the effect of screening in the low q region. However, to fit the experimental behavior of λ_g in this region by adjusting τ_b^{-1} would require an unjustifiable order of magnitude increase in boundary scattering.

The data for the most heavily doped sample of Challis et al.[2] are shown in Fig. 4 with data for the three samples described here. The data for Challis's sample number 6 was analyzed using the method outlined here with the result for the values of the parameters: $C = -1.25$ eV, $d = 16.5^{o}K^{-4}sec^{-1}$, $\theta^* = 15.5^{o}K$, and $q_{TF}^{e} = 0.87 \times 10^{6}$ cm^{-1}. These values are in good agreement with the values for samples A, B and C presented in Table II.

A number of other possible explanations for the discrepancy between experimental and theoretical values of q_{TF} or for partial compensation of the effect of screening have been examined. The case of additional bands of scatterers lends itself to a relatively simple study using the formalism already developed.

Awareness of the fact that semimetals such as antimony, which have many similarities to degenerate semiconductors, show only a limited amount of screening was a clue in the search for a reason for the unexpectedly small empirical values of q_{TF}. Usually in semimetals, carrier compensation is cited as the cause for the absence of screening, even though a less restrictive condition such as the existence of multiple bands without compensation would be sufficient to diminish the screening. In this respect, there are two possibilities for an additional band in the samples under study; firstly, an impurity band[35] and secondly, the light hole band

which is degenerate with the principal heavy hole band at the center of the zone.

In the case where $|B| \gg |\sigma_1'|$, which is roughly equivalent to $q > q_{TF}$, Eq. (26) gives

$$\Omega(q) = \frac{q^2}{\rho e^2 s^2} \mathrm{Re}(\sigma_1 C_1^2 + \sigma_2 C_2^2) \tag{34}$$

independently of the sign of the carriers in the two bands. However, for small q where $|B| \ll |\sigma_1'|$, the resulting expression is

$$\Omega(q) = \frac{q^2}{\rho e^2 s^2} \mathrm{Re} \frac{\sigma_1 \sigma_2 (C_1 \pm C_2)^2}{\sigma_1 + \sigma_2} \quad , \tag{35}$$

where the positive sign is appropriate for bands of carriers whose charges are opposite. Assuming that the impurity band[37] could be treated as a normal conducting band of electrons the positive sign in Eq. (35) would apply and the effect of going from $q \gg q_{TF}$ to $q \ll q_{TF}$ would amount to a step down (or up) in the linearly varying scattering frequency by a ratio of approximately σ_2' to σ_1'. This is in contrast to the extremely rapid ($>q^3$) fall in $\Omega(q)$ below q_{TF} in the case of a single band.

Should one instead consider the case of the light hole band, the negative sign applies and, owing to the near equality of C_1 and C_2 in this case due to the degeneracy of the bands at the center of the zone, the scattering frequency is negligible. Thus the light hole band does not appear to assist in explaining the added

scattering.

No attempt was made to use Eq. (34) and Eq. (35) to analyze the data under the impurity band hypothesis due to the additional unknown parameters, but it may be seen that this process would work in the desired direction to compensate for the screening.

VI. CONCLUSIONS

It has been shown that the lattice thermal conductivity of degenerate p-type InSb at helium temperatures can be successfully accounted for with a phenomenological model in which a principal phonon scattering mechanism is due to charge carriers. The other mechanisms included in this model are Rayleigh scattering due to impurities and isotopes and boundary scattering.

This model with emphasis on carrier-phonon scattering has been chosen in preference to a model with an interaction of the type proposed by Keyes.[30] The type of scattering proposed by Keyes would yield curves of similar shapes to those in Fig. 2. However, these would not merge toward a common value at the lower temperatures. The cutoff in the Keyes model, as discussed in the theory section, should also be independent of the impurity concentration. Also in favor of carrier-phonon scattering over impurity scattering are the recent results of Shalyt et al.[38] shown in Fig. 4 who obtained the same conductivity for two n-type samples with the same carrier concentrations but different acceptor-donor concentrations. This indicates that the scattering is dependent on the free carrier concentration rather than the concentration of impurities.

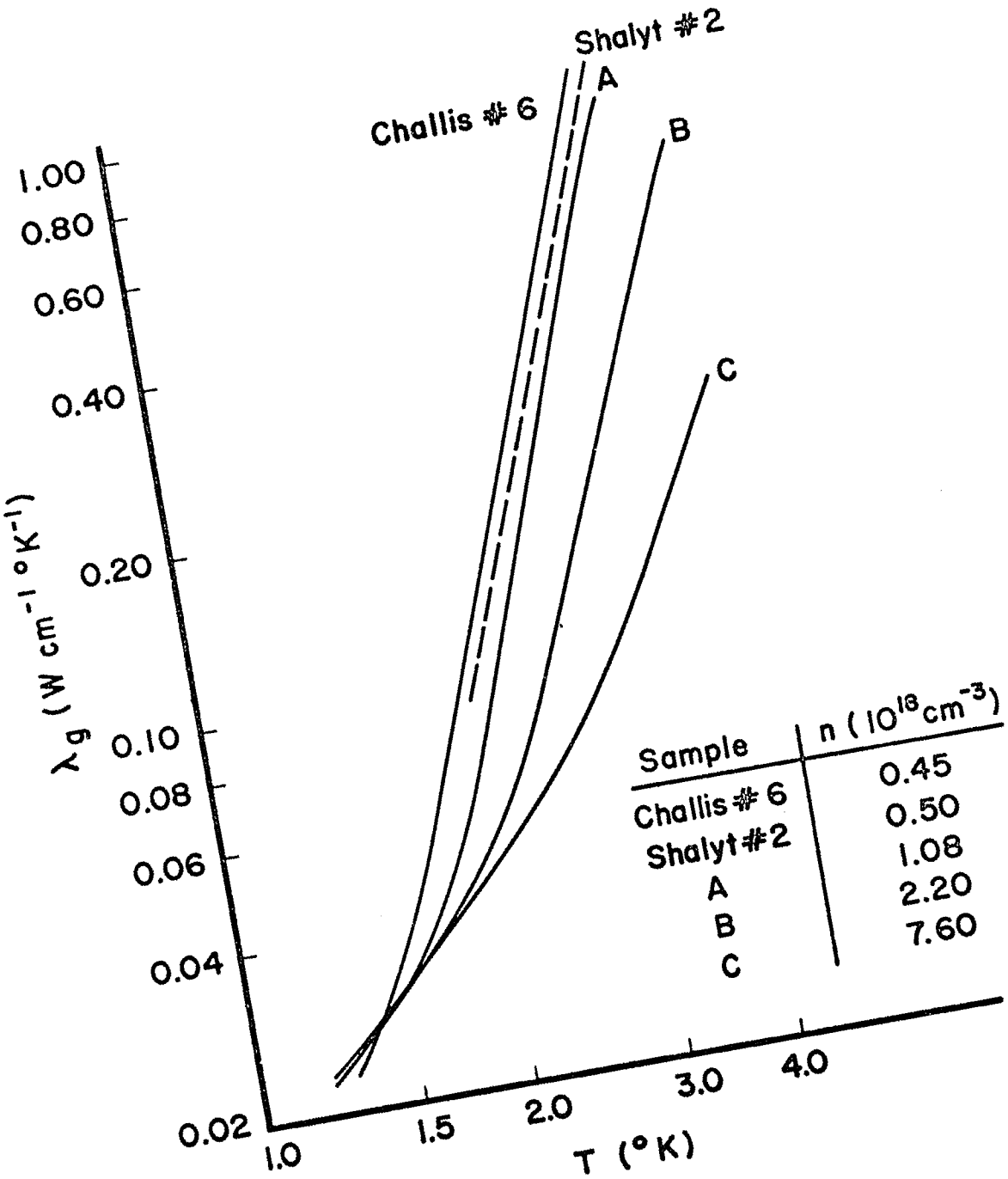
Shalyt #2
A
Challis #6
B
C
1.00
0.80
0.60
0.40
0.20
0.10
0.08
0.06
0.04
0.02
λg (W cm⁻¹ °K⁻¹)
1.0
1.5
2.0
3.0
4.0
T (°K)
Sample
n (10¹⁸cm⁻³)
Challis #6
0.45
Shalyt #2
0.50
A
1.08
B
2.20
C
7.60

Fig. 4

REFERENCES

1. R. S. Blewer, N. H. Zebouni, and C. G. Grenier, Phys. Rev. 174, 700 (1968).
2. L. J. Challis, J. D. Cheeke, and D. J. Williams, in Proceedings of the Ninth International Conference on Low Temperature Physics (Plenum Press, New York, 1965), p. 1145.
3. M. H. Cohen, M. J. Harrison, and W. A. Harrison, Phys. Rev. 117, 937 (1960).
4. M. J. Harrison, Phys. Rev. 119, 1260 (1960).
5. H. N. Spector, Phys. Rev. 127, 1084 (1962).
6. H. N. Spector, in Solid State Physics, edited by F. Seitz and D. Turnbull (Academic Press, New York, 1966), Vol. 19, p. 291.
7. A. B. Pippard, Phil. Mag. 46, 1104 (1955); Proc. Roy. Soc. (London) A257, 165 (1961).
8. Nobuo Mikoshiba, J. Phys. Soc. Japan 12, 1691 (1959); 15, 982 (1960); 16, 895 (1961).
9. E. I. Blount, Phys. Rev. 114, 418 (1959).
10. S. G. Eckstein, Phys. Rev. 131, 1087 (1963).
11. M. G. Holland, Phys. Rev. 134, A471 (1964).
12. J. A. Carruthers, T. H. Geballe, H. M. Rosenberg, and J. M. Ziman, Proc. Roy. Soc. (London) A238, 502 (1957).
13. J. A. Carruthers, J. F. Cochran, and K. Mendelssohn, Cryogenics 2, 160 (1962).

14. Cominco American Inc., Spokane Industrial Park, Spokane, Washington 99216.

15. J. R. Long, Ph.D. dissertation, Louisiana State University, 1965 (unpublished).

16. Leeds & Northrup Company, Sumneytown Pike, North Wales, Pennsylvania 19454.

17. Honeywell, Test Instrument Division, 4800 E. Dry Creek Road, Denver, Colorado 80217.

18. Keithley Instruments, Inc., 28775 Aurora Road, Cleveland Ohio 44139.

19. Materials Used in Semiconductor Devices, edited by C. A. Hogarth (Interscience Publishers, New York, 1965), pp. 135, 150.

20. There is a consensus (Refs. 21-24) of results which indicates that the values of n listed in Table I and used in the calculations throughout this work should be increased by a factor of between 1.3 and 1.5. The quantities which would be affected by an increase in the carrier density are τ_e, ℓ, k_F, c, d, and θ^*.

21. Gaston Fischer, Helv. Phys. Acta 33, 463 (1960).

22. H. J. Hrostowski, F. J. Morin, T. H. Geballe, and G. H. Wheatley, Phys. Rev. 100, 1672 (1955).

23. H. P. R. Frederikse and W. R. Hosler, Phys. Rev. 108, 1146 (1957).

24. C. H. Champness, Phys. Rev. Letters 1, 439 (1958).

25. Joseph Callaway, Phys. Rev. 113, 1046 (1959); 122, 787 (1961).

26. R. F. Potter, Phys. Rev. 103, 47 (1956).

27. H. B. G. Casimir, Physica 5, 495 (1938).

28. P. G. Klemens, in Solid State Physics, edited by F. Seitz and D. Turnbull (Academic Press, New York, 1958), Vol. 7, p. 1.

29. R. O. Pohl, Phys. Rev. Letters 8, 481 (1962).

30. R. W. Keyes, Phys. Rev. 122, 1171 (1961).

31. J. M. Ziman, Phil. Mag. 1, 191 (1956); Electrons and Phonons, (Oxford University Press, London, 1960), pp. 329-330.

32. E. H. Sondheimer, Proc. Phys. Soc. (London) A65, 561 (1952).

33. Usually $\alpha = 1$ unless the recombination strongly depends on compressive deformation and the recombination time is short. The dependence of α on ω has not been developed in view of the uncertainties involved. Even though computations were made with values of α other than unity, the final analysis uses $\alpha = 1$ only.

34. E. F. Steigmeir and B. Abeles, in Proceedings of the Seventh International Conference on the Physics of Semiconductors, (Academic Press, New York, 1965), p. 701.

35. For acceptor doping levels such that indium antimonide is degenerate at liquid helium temperatures, it is expected that an "impurity band" is formed in which there could be a conduction mechanism at least as efficient as the hopping of electrons from one impurity site to another. The carriers in this band, which for acceptor impurity concentrations above 2×10^{17} cm^{-3} overlaps the valence band (Ref. 32) have a small conductivity which should increase with increased doping.

36. R. F. Broom and A. C. Rose-Innes, Proc. Phys. Soc. (London) B69, 1269 (1956).

37. The condition $\sigma_2^o < \sigma_1^o$ does not induce the same relationship between the σ_i. For the impurity band, the conditions $q\ell_2 < q\ell_1$ and $\omega\tau_2 < \omega\tau_1$ may yield values of σ_1' and σ_2' of comparable magnitude. It is expected that in the present case $\sigma_2' < \sigma_1'$ where index 1 refers to the heavy hole band and index 2 refers to the impurity band.

38. S. S. Shalyt, P. V. Tamarin, and V. S. Ivleva, Phys. Letters 32A, 29 (1970).

VITA

Charles Richard Crosby was born July 15, 1934 in Oklahoma City, Oklahoma. He was graduated from high school in Warren County, Mississippi in 1953, whereupon he entered Hinds Junior College in Raymond, Mississippi. In 1955 he entered Louisiana State University as a junior. He received the degrees of Bachelor of Science and Master of Science from this institution in 1957 and 1960 respectively. After a four year period in which he was employed in the Central Research Laboratories of Texas Instruments Inc. of Dallas, Texas he re-entered the Graduate School of Louisiana State University. He is presently a candidate for the degree of Doctor of Philosophy in the Department of Physics and Astronomy of Louisiana State University.

EXAMINATION AND THESIS REPORT

Candidate: Charles Richard Crosby

Major Field: Physics

Title of Thesis: Thermal Conductivity of Heavily Doped p-Type InSb at Liquid Helium Temperatures.

Approved:

Claude J. Gruninger
Major Professor and Chairman

Max Goodrich
Dean of the Graduate School

EXAMINING COMMITTEE:

John T. Marshall

Robert D. Hussey

G. H. Thomas

James E. Keister

Date of Examination:

April 13, 1971